Geosci. Model Dev. Discuss., https://doi.org/10.5194/gmd-2018-41
Manuscript under review for journal Geosci. Model Dev.
Discussion started: 15 March 2018

Geoscientific Model Development Discussions

Carbon-nitrogen coupling under three schemes of model representation: Traceability analysis

Zhenggang Du[1,2], Ensheng Weng[3], Jianyang Xia[1,2*], Lifen Jiang[4], Yiqi Luo[4,5], Xuhui Zhou[1,2,6*]

[1]*Center for Global Change and Ecological Forecasting, School of Ecological and Environmental Sciences, East China Normal University, Shanghai 200062, China*

[2]*Tiantong National Field Observation Station for Forest Ecosystem, School of Ecological and Environmental Sciences, East China Normal University, Shanghai 200062, China*

[3]*Department of Ecology & Evolutionary Biology, Princeton University, Princeton, NJ, USA*

[4]*Center for Ecosystem Science and Society, Northern Arizona University, AZ, USA*

[5]*Department for Earth System Science, Tsinghua University, Beijing 100084, China*

[6]*Shanghai Institute of Pollution Control and Ecological Security, 1515 North Zhongshan Rd, Shanghai 200437, China*

***For correspondence:**

Xuhui Zhou

School of Ecological and Environmental Sciences

East China Normal University

500 Dongchuan Road, Shanghai 200062, China

Email: xhzhou@des.ecnu.edu.cn

Tel/Fax: +86 21 54341275

Jianyang Xia

School of Ecological and Environmental Sciences

Geosci. Model Dev. Discuss., https://doi.org/10.5194/gmd-2018-41
Manuscript under review for journal Geosci. Model Dev.
Discussion started: 15 March 2018

East China Normal University

500 Dongchuan Road, Shanghai 200062, China

Email: jyxia@des.ecnu.edu.cn

Geosci. Model Dev. Discuss., https://doi.org/10.5194/gmd-2018-41
Manuscript under review for journal Geosci. Model Dev.
Discussion started: 15 March 2018

Geoscientific Model Development Discussions

Abstract The interaction between terrestrial carbon (C) and nitrogen (N) cycles has been incorporated into more and more land surface models. However, the scheme of C-N coupling differs greatly among models, and how these diverse representations of C-N interactions will affect C-cycle modeling remains unclear. In this study, we explored how the simulated ecosystem C storage capacity in the terrestrial ecosystem (TECO) model varies with three different commonly-used schemes of C-N coupling. The three schemes (SM1, SM2, and SM3) have been used in three different coupled C-N models (i.e., TECO-CN 2.0, CLM 4.5, and O-CN, respectively). They differ mainly in the stoichiometry of C and N in vegetation and soils, plant N uptake strategies, pathways of N import, and the competition between plants and microbes for soil mineral N. We incorporated them into the C-only version of TECO model, and evaluated their impacts on the C cycle with a traceability framework. Our results showed that all of the three C-N schemes resulted in significant reductions in steady-state C storage capacity compared with the C-only version, but the magnitude varied with -23%, -30% and -54% for SM1, SM2, SM3, respectively. The reduced C storage capacity is the combination of decreases in net primary productivity (NPP) by -29%, -15% and -45% with changes of mean C residence time (MRT) by 9%, -17% and -17% for SM1, SM2, and SM3, respectively. The divergent NPP are mainly attributed to the different assumptions on plant N uptake, plant tissue C:N ratio, down-regulation photosynthesis, and biological N fixation. In comparison, the alternative representations of the plant and microbe competition strategy and the plant N uptake, combining with the flexible C:N ratio in vegetation and soils, led to a notable spread MRT. These results highlight that the diverse assumptions on N process representation among different C-N coupled models could cause additional uncertainty to land surface models. Understanding their difference can help us to improve the capability of models to predict future biogeochemical cycles on land.

Keywords: carbon-nitrogen coupling, traceability analysis, carbon storage capacity, nitrogen limitation, carbon residence time

Geosci. Model Dev. Discuss., https://doi.org/10.5194/gmd-2018-41
Manuscript under review for journal Geosci. Model Dev.
Discussion started: 15 March 2018

1. Introduction

The terrestrial ecosystem carbon (C) storage is jointly determined by ecosystem C input (i.e., net primary productivity, NPP) and mean residence time (MRT), which are modulated by the availability of nitrogen (N) for plant and microbial growth (Vitousek et al., 1991; Wieder et al., 2015; Luo et al., 2017). N is an essential component of enzymes, proteins, and secondary metabolites (van Oijen and Levy, 2004). Plant production require N to meet the stoichiometric demands (Cleveland et al., 2013). Although there is abundant N in the atmosphere, it is difficult to make it available for biological systems (Houlton et al., 2008). As a consequence, the biological N availability, which strongly affects C storage in ecosystems, is often highly correlated with key metabolic rates such as photosynthesis (Field and Mooney, 1986; Du et al., 2017) and respiration (Sprugel et al., 1996). N thus plays an important role in governing the C balance and turnover of terrestrial ecosystem (García-Palacios et al., 2013; Shi et al., 2015).

Given the importance of N availability on C sink projections (Wang and Houlton 2009, Zaehle et al., 2015, Wieder et al., 2015), N processes are increasingly incorporated into biogeochemical models. The representation of N cycling and their feedback to C cycling in models reflects what has been established in the ecosystem research community. Early C-N coupled models demonstrated that the N availability limits C storage capacity and can lead to growth enhancement when N mineralization increases in many terrestrial ecosystems (i.e., progressively increasing N limitation) (Melillo et al., 1993; Luo et al., 2004). Evidences from more recently studies have largely confirmed these results and have generated multiple hypotheses for improving C-N coupling models (Zhou et al., 2013; Zaehle et al., 2014; Thomas et al., 2015). They include the plant down-regulation productivity based on N required for cell construction or N availability for plant absorption (Thornton et al., 2009; Gerber et al., 2010), constant or flexible stoichiometry for allocation and tissue (Wang et al., 2001; Shevliakova et al., 2009; Zaehle et al., 2010), competition between plants and microbes for soil nutrients (Zhu et al., 2017), Evapotranspiration- or NPP-driven empirical functions to generate spatial estimates of biological N fixation (BNF) (Wieder et al., 2015), and respiration of excess C to obtain N from environment and/or to prevent the accumulation of C beyond the storage capacity (Zaehle et al., 2010). These knowledge have significantly helped improve our understanding of the terrestrial C-N coupling and are an important basis to develop comprehensive terrestrial process-based

models (Thornton et al., 2007; Thomas et al., 2013). However, simulated results of the terrestrial C cycle illustrated considerable spread among models, and much of uncertainty arose from predictions of N effects on C dynamic. The contradictory results were largely from different representations of fundamental N processes (e.g., the degree of flexibility of C:N ratio in vegetation and soils, plant N uptake strategies, pathways of N export, decomposition, and the representations of the competition between plants and microbes for mineral N). Furthermore, the methodology used to derive the C-N coupling schemes among models varies largely, which may be invalid for the model intercomparisons to provide insight into the underlying mechanism of N status for terrestrial C cycle projection.

In the past decades, terrestrial models integrated more and more processes to improve model performance. While the more processes incorporated, the more difficult it becomes to understand or evaluate model behavior (Luo et al., 2015). Xia et al (2013) developed a traceability analysis framework that helped improve the comparability of models and data, evaluated impacts of additional model components, facilitated benchmark analyses, model intercomparisons, and data-model fusion, and improved model predictive power. Based on the traceability analysis framework, key traceable elements, including fundamental properties of the terrestrial C cycle and their representation in shared structures among existing models, can be identified and characterized under different sources of variation (e.g., external forcing and uncertainty in processes) compared to the achieved predictive ability. The traceability analysis framework enables diagnosis of where models are clearly lacking predictive ability and evaluation of the relative benefit when more or alternative components are added to the models (Luo et al., 2015).

The present study is designed to examine the effects of C-N coupling under different schemes of model representation on ecosystem C storage in the Terrestrial Ecosystem (TECO) model with traceability analysis framework. Three schemes of model representation were conducted mainly based on TECO-CN 2.0 (SM1), CLM 4.5 (SM2), and O-CN (SM3, Table 1). The three C-N schemes differ in degrees of flexibility of C:N ratio in vegetation and soils, plant N uptake strategies, pathways of N import, and the representations of the competition between plants and microbes for soil available N. Based on the forcing data of ambient CO_2 concentration, N deposition and meteorological data (i.e., air temperature, soil temperature, relative humidity, vapour pressure deficit, precipitation, wind speed, photosynthetically active radiation) obtained from Duke Forest during the period of 1996-2007, we conduct three alternative C-N coupling

schemes (i.e., SM1, SM2 and SM3) as well as C-only in TECO model framework to compare their effects on the ecosystem C storage capacity using traceability analysis framework. The N-processes sensitivity analysis was carried out to evaluate the variability in estimated ecosystem C storage caused by the process-related parameters at steady state.

2. Materials and methods

2.1 Data sources

The forcing data used in this study were taken from the AmeriFlux site at Duke Forest, located in the Blackwood Division, North Carolina, USA (35.97^{o} N, 79.08^{o} W). The flux tower lies on a 15-year-old loblolly pine (*Pinus taeda L.*) plantation. The meteorological forcing data were downloaded from the AmeriFlux database at http://ameriflux.lbl.gov, including ambient CO_2 concentration ($[CO_2]$), air temperature at the top canopy (*Ta*), soil temperature (*Ts*), photosynthetically active radiation (*PAR*), relative humidity (*RH*), vapor pressure deficit (*VPD*), precipitation, wind speed [*Ws*], and N deposition. All forcing data sets are available from 1996 to 2007. Standing biomass and biomass production date at each plot for plant compartments (i.e., foliage, fine root and woody biomass, including branches and coarse roots) were taken from McCarthy et al. (2010). The C and N concentration data for each plant compartment based on Finzi et al. (2007) were used to estimate C and N stocks and fluxes. Plant N demand and uptake were calculated from these data following Finzi et al. (2007). The C and N concentrations of litter and SOM were obtained from Lichter et al. (2008).

2.2 Model description and C-N schemes

2.2.1 TECO-CN 2.0

The terrestrial ecosystem C-N coupling model (TECO-CN, version 2.0) used in the present study is a variant of the TECO-Carbon-only version (TECO-C) by incorporating additional key N processes (Figure 1). TECO-C model is a process-based ecosystem model designed to examine critical processes regulating interactive responses of plants and ecosystems to climate change. It has four major components: canopy photosynthesis module, plant growth module, soil water dynamic module, and soil C dynamic module. The canopy photosynthesis and soil water dynamic modules run at hourly time step while the plant growth and soil C dynamic modules run

Geosci. Model Dev. Discuss., https://doi.org/10.5194/gmd-2018-41
Manuscript under review for journal Geosci. Model Dev.
Discussion started: 15 March 2018

at the daily time step. The detailed description of the TECO-C model can be found in Weng and Luo (2008).

The N cycle added to the TECO model for this study is simplified following the structure of Luo & Reynolds (1999), Gerber et al. (2010), and Wang et al. (2010). It has a similar structure to the TECO-C model (Figure 1). There are nine organic N pools and one inorganic soil N pool, including plant, litter and soil N pools. The plant N pools include leaves, wood, roots, and mineral N in plant tissues. The litter and soil N pools include metabolic and structural litter N, fast, slow, and passive soil organic N (SON), and soil mineral N pools. The total plant N demand on each time step is calculated following the NPP allocation to new tissue growth based on their C:N ratios. To meet the demand, the plant N supply is calculated from three parts, including the retranslocated N from senescing tissues, plant uptake from soil mineral N pool, and external N sources from atmospheric deposition and biological N fixation. The N absorbed by roots enters into the mineral N pool in plant tissues, and then is allocated to the remaining plant pools with plant growth. The N in leaves and fine roots is reabsorbed before senescence. Plant litters will enter metabolic or structural pools depending on their C:N ratios.

Allocation of assimilated C among the leaves, stems and roots depends on their growth rates, and varies with phenology (Luo et al., 1995; Denison and Loomis, 1989; Shevliakova et al., 2009; Weng and Luo, 2008):

$$b_l = \frac{1}{1+c_1+c_2} \quad (1)$$

$$b_s = \frac{c_2}{1+c_1+c_2} \quad (2)$$

$$b_r = \frac{c_1}{1+c_1+c_2} \quad (3)$$

where b_l, b_s and b_r are the partitioning coefficient of newly assimilated C to leaves, stems and roots, respectively. Parameters c_1 and c_2 are calculated as:

$$c_1 = \frac{bm_l}{bm_r} * \frac{CN_l^i}{CN_l^0} \quad (4)$$

$$c_2 = 0.5 * 250e^3 * SLA * 0.00021 * h^2 \quad (5)$$

where bm_l and bm_r are the leaf and root biomass; CN_l^i and CN_l^0 represent the C:N ratio of the leaf pool at 0 and current time step, respectively; SLA is specific leaf area; h is plant height, which is calculated as:

$$h = h_{max}(1 - \exp(-h_1 * bmP)) \quad (6)$$

Geosci. Model Dev. Discuss., https://doi.org/10.5194/gmd-2018-41
Manuscript under review for journal Geosci. Model Dev.
Discussion started: 15 March 2018

where h_{max} is the maximum canopy height; h_1 is an empirical parameter and bmP is plant biomass.

2.2.2 C-N coupling schemes

We conducted four experiments including three simulations with their representations of C-N coupling schemes (SM1, SM2 and SM3) and an additional C-only simulation in TECO model framework. The three C-N interaction simulations include one original scheme in TECO-CN2.0 model and the other two schemes representing CLM4.5-BGC and O-CN. The three C-N coupling schemes differ in the representation of down-regulation of photosynthesis, the degree of flexibility of C:N ratio in vegetation and soils, plant N uptake strategies, pathways of N import to the plant reserves, and the competition between plants, and microbes for soil mineral N (Table1, Figure 2).

SM1 (TECO-CN2.0)

The N down-regulation of photosynthesis in SM1 is determined by the comparison between plant N demand and actual supply of N:

$$f_{dreg} = \min(\frac{N_{sup}}{N_{demand}}, 1) \quad (7)$$

where N_{demand} is plant N demand, and N_{sup} is actual supply of N obtained from re-translocated N, plant N uptake, and biological N fixation.

The re-translocated N is calculated as:

$$N_{retrans} = \sum_{i=leaf,wood,root} r_i \times outC_i/CN_i \quad (8)$$

where r_i is the N resorption coefficient and $outC_i$ is the value of C leaving plant pool *i* in each time step.

The plant N uptake from soil mineral N pool is a function of root biomass density ($Root_{total}$, g C m^{-2}) and N demand of plants, following McMurtrie *et al*. (2012)

$$N_{uptake} = min(\max(0, N_{demand} - N_{retrans}), f_{U,max} \times SN_{mine} \times \frac{Root_{total}}{Root_{total}+Root_0}) \quad (9)$$

where N_{demand} is the N demand of plants; SN_{mine} is the soil mineral N (gN m^{-2}); $f_{U,max}$ is the maximum rate of N absorption per step when $Root_{total}$ approaches infinity; and $Root_0$ is a constant of root biomass (g C m^{-2}) at which the N-uptake rate is half of the parameter $f_{U,max}$.

The biological N fixation is calculated as:

Geosci. Model Dev. Discuss., https://doi.org/10.5194/gmd-2018-41
Manuscript under review for journal Geosci. Model Dev.
Discussion started: 15 March 2018

$$N_{BNF} = \min(\max(0, N_{demand} - N_{retrans} - N_{uptake}), n_{fix} \times f_{nsc} \times NSC) \quad (10)$$

where $n_{fix} = 0.0167$ is the maximum N fixation ratio and f_{nsc} is the nutrient concentration limiting factor. f_{nsc} is calculated as

$$f_{nsc} = \begin{cases} 0, & NSC < NSC_{min} \\ \frac{NSC - NSC_{min}}{NSC_{max} - NSC_{min}}, & NSC_{min} < NSC < NSC_{max} \\ 1, & NSC > NSC_{max} \end{cases} \quad (11)$$

where NSC_{min} and NSC_{max} are the minimal and maximal sizes of nonstructural C pool, respectively.

Two pathways of N loss are modeled. One is gaseous loss and another is leaching. They both are proportional to the availability of soil mineral N (SN_{min}). The equations are:

$$N_{gas\_loss} = f_{ngas} \times e^{\frac{T_{soil}-25}{10}} \times SN_{min} \quad (12)$$

$$N_{leach} = f_{nleach} \times \frac{V_{runoff}}{h_{depth}} \times SN_{min} \quad (13)$$

where $f_{ngas} = 0.001$ and $f_{nleach} = 0.5$, T_{soil} is the soil temperature, V_{runoff} is the value of runoff, and h_{depth} is the soil depth.

SM2 (CLM4.5bgc)

The N down-regulation of photosynthesis in SM2 is calculated as:

$$f_{dreg} = \frac{CF_{allo} - CF_{avail\_alloc}}{CF_{GPP_{pot}}} \quad (14)$$

where CF_{allo} is the total flux of allocated C, which is determined by available mineral N. CF_{avail_alloc} is the potential C flux from photosynthesis, which can be allocated to new growth. $CF_{GPP_{pot}}$ is the potential gross primary productivity (GPP) when there no N limitation.

The re-translocated N is calculated as:

$$N_{retrans} = \min(N_{demand} \times \frac{N_{retrans_{ann}}}{N_{demand_{ann}}}, N_{retrans\_avail}) \quad (15)$$

where $N_{retrans_{ann}}$ is the previous year's annual sum of re-translocated N obtained from senescing tissues, $N_{demand_{ann}}$ is the previous year's annual sum of plant N demand. $N_{retrans\_avail}$ is the available re-translocated N in senescing tissues, which is calculated by the proportional of senescing tissues.

The plant N uptake is described as:

Geosci. Model Dev. Discuss., https://doi.org/10.5194/gmd-2018-41
Manuscript under review for journal Geosci. Model Dev.
Discussion started: 15 March 2018

$$N_{uptake} = (N_{demand} - N_{retrans}) \times f_{plant\_demand} \quad (16)$$

where f_{plant_demand} is the fraction (from 0 to 1) of the plant N demand, which can be met given the current soil mineral N supply and competition with heterotrophs. f_{plant_demand} is set equal to the fraction of potential immobilization demand (f_{immob_demand}) that is calculated as:

$$f_{plant\_demand} = f_{immob\_demand} = \frac{SN_{min}}{N_{plant\_demand}+N_{immob\_demand}} \quad (17)$$

where N_{immob_demand} is the total potential N immobilization demand (i.e., total potential microbial N demand).

The biological N fixation is calculated as:

$$N_{BNF} = {1.8(1 - e^{-0.03\times NPP_{py}})}\Big/{(86400 \times 365)} \quad (19)$$

where NPP_{py} is the previous year NPP.

SM3 (O-CN)

The N downregulation of photosynthesis in SM3 is calculated as:

$$f_{dreg} = a + b \times N_{leaf/LAI} \quad (20)$$

where a and b are empirical constants, and $N_{leaf/LAI}$ is foliage N per unit leaf area.

The re-translocated N is calculated as:

$$N_{retrans} = \sum_{i=leaf,root} \tau_i \times f_{trans,i} \quad (21)$$

where τ is the foliage or roots shed each step. $f_{trans,leaf} = 0.5$ and $f_{trans,root} = 0.2$ are the fractions of N re-translocated when the tissue dying off.

The plant N uptake is calculated as:

$$N_{uptake} = v_{max} \times SN_{min} \times \left(k_{Nmin} + \frac{1}{N_{min}\times K_{Nmin}}\right) \times f(T_{soil}) \times f(NC_{plant}) \times C_{root} \quad (22)$$

where v_{max} is maximum N uptake capacity per unit fine root mass, k_{Nmin} is the rate of N uptake not associated with Michaelis-Menten Kinetics, K_{Nmin} is the half saturation concentration of fine root N uptake. $f(T_{soil})$ is calculated as:

$$f(T_{soil}) = \exp\left(308.56 * \left(\frac{1}{56.02} - \frac{1}{T_{soil}+46.02}\right)\right) \quad (23)$$

where T_{soil} is soil temperature.

Geosci. Model Dev. Discuss., https://doi.org/10.5194/gmd-2018-41
Manuscript under review for journal Geosci. Model Dev.
Discussion started: 15 March 2018

C_{root} is fine root mass. $f(NC_{plant})$ is the dependency of N uptake on plant N status, and is calculated as:

$$f(NC_{plant}) = \max(\frac{NC_{plant}-nc_{leaf,max}}{nc_{leaf,min}-nc_{leaf,max}}, 0) \quad (24)$$

where $nc_{leaf,min}$ and $nc_{leaf,max}$ are the minimum and maximum foliage N concentrations, respectively. NC_{plant} is taken as the mean N concentration of foliage, fine roots, and labile N pools, representing the active and easily translocatable portion of plant N:

$$NC_{plant} = \frac{N_{leaf}+N_{root}+N_{labile}}{C_{leaf}+C_{root}+C_{labile}} \quad (25)$$

The biological N fixation is calculated as:

$$N_{BNF} = 0.1 \times \max(0.0234 \times 30 \times AET + 0.172, 0) \quad (26)$$

where *AET* is the mean annual evapotranspiration.

2.3 Traceability analysis framework

The traceability analysis framework was used to evaluate the variation of the modeled ecosystem C storage capacity under different C-N schemes (Figure S1). According to the traceability analysis framework (Xia et al., 2013), the modeled C storage capacity can be traced to (i) a product of NPP and ecosystem residence time (τ_E). The latter τ_E can be further traced to (ii) baseline C residence time (τ_E'), which is usually preset in a model according to vegetation characteristics and soil types, (iii) N scalar (ξ_N), (iv) environmental scalars (ξ) including temperature (ξ_T) and water (ξ_W) scalars, and (v) the external climate forcing. The framework for decomposing modeled C storage capacity into a few traceable components is built upon a pool- and flux- structure, which is adopted in all of the terrestrial C models. The structure can well be represented by a matrix equation (Luo et al., 2003; Luo and Weng, 2011):

$$\frac{dX(t)}{dt} = BU(t) - A\xi CX(t) \quad (27)$$

where $X(t) = (X_1(t), X_2(t), \dots, X_8(t))^T$ is an 8 × 1 vector describing eight C pool sizes in leaf, root, wood, metabolic litter, structural litter, fast, slow, and passive soil organic C, respectively, in the TECO model (Weng and Luo, 2008). $B = (b_1,\ b_2, b_3, 0, \dots, 0)^T$ represents the partitioning coefficients of the photosynthetically fixed C into different plant pools. *U(t)* is the input of fixed C via plant photosynthesis. *A* is an 8 × 8 matrix representing the C transfer between pools. ξ is an 8 × 8 diagonal matrix of control of plant N status and environmental scalars on C decay rate at

Geosci. Model Dev. Discuss., https://doi.org/10.5194/gmd-2018-41
Manuscript under review for journal Geosci. Model Dev.
Discussion started: 15 March 2018

each time step. *C* is an 8 × 8 diagonal matrix representing the C exit rates from a pool at each time step.

The C storage capacity equals the sum of C in all pools at steady state (X_{ss}), which can be obtained by making Eqn.(27) equal zero as described in Xia et al. (2013):

$$X_{ss} = (A\xi C)^{-1}BU_{ss} \quad (28)$$

The vector U_{ss} is the ecosystem C influx at steady state. The partitioning (*B* vector), transfer coefficients (*A* matrix) and exit rates (*C* matrix) in Eqn.(27) together determine the baseline C residence time (τ_E'):

$$\tau_E' = (AC)^{-1}B \quad (29)$$

The baseline C residence time (τ_E') in Eqn.(29), N scalars (ξ_N) and environmental scalars (ξ_E) values together determine the C residence time (τ_E):

$$\tau_E = \xi^{-1}\tau_E' = (\xi_N \times \xi_E)^{-1}\tau_E' \quad (30)$$

Thus, the C storage capacity is jointly determined by the ecosystem residence time (τ_E) and steady state C influx (U_{ss}):

$$X_{ss} = \tau_E U_{ss} \quad (31)$$

The environmental scalar is further separated into the temperature (ξ_T) and water (ξ_W) scalar components, which can be represented as:

$$\xi_E = \xi_T \times \xi_W \quad (32)$$

The N scalar is given by vector $\xi_N = (\xi_{N1}(t),\ \xi_{N2}(t), \dots, \xi_{N8}(t))^T$. The component $\xi_{Ni}(t)$ quantifies the changes of N content at each time step compared with initial condition in the plant pool *i*. It is calculated as:

$$\xi_{Ni} = \exp\left(-\frac{CN_i^0 - CN_i^n}{CN_i^0}\right) \quad (33)$$

where CN_i^0 and CN_i^n are the C:N ratio of the pool *i* at 0 and *n* time step, respectively.

2.4 Model simulations and sensitivity analysis

To obtain the modeled C storage capacity, we spun up the TECO model with the C-only and three C-N coupling schemes to steady state using the semi-analytical solution method developed by Xia et al. (2012). Once the simulations are spun up to steady state, C and N fluxes and state variables as well as the matrix elements *A*, *C*, *B*, and ξ in Eqn.(28) from all time steps in the last recycle of the climate forcing were saved for traceability analysis.

Geosci. Model Dev. Discuss., https://doi.org/10.5194/gmd-2018-41
Manuscript under review for journal Geosci. Model Dev.
Discussion started: 15 March 2018

The sensitivities of both NPP and MRT to each main N process in three schemes were calculated as:

$$S_i^{NPP}(P) = \frac{NPP_i^+(P) - NPP_i^-(P)}{NPP_i^0} \quad (34)$$

$$S_i^{MRT}(P) = \frac{MRT_i^+(P) - MRT_i^-(P)}{MRT_i^0} \quad (35)$$

where $S_i^{NPP}(P)$ and $S_i^{CRT}(P)$ $(i = 1, 2, 3)$ represent the sensitivities of the NPP and MRT to the N-process P in the scheme i, respectively. $NPP_i^+(P)$ and $NPP_i^-(P)$ are the annual mean values of NPP that were simulated in scheme i based on the value of the N-process P (ie., DRP, PS, PUN, PMC, BNF, RtrN and SS) increasing 50% and decreasing 50%, respectively. $MRT_i^+(P)$ and $MRT_i^-(P)$ are the annual mean values of MRTs that were simulated in the same way as NPP and calculated using Eqn.(29) and Eqn.(30). NPP_i^0 and MRT_i^0 are the annual mean values of NPP and MRT at the steady state in the scheme i.

3. Results

3.1 Simulations of C and N dynamics at steady state

At the steady state, the dynamics of N fluxes and soil mineral N showed different patterns among three C-N schemes in the TECO model (Fig 3). The simulated soil N mineralization and plant N uptake fluxes in SM2 displayed the largest daily variations (0.0015 and 0.00086 g N $m^{-2}d^{-1}$, respectively) and annual mean values (1.26 and 0.23 g N $m^{-2}yr^{-1}$, respectively) among three C-N schemes. For the N leaching flux, SM1 showed the largest daily variation (0.04 g N $m^{-2}d^{-1}$) and annual mean value (0.36 g N $m^{-2}yr^{-1}$). However, the biological N fixation (BNF) flux in SM1 showed the largest daily variation (0.028 g N $m^{-2}d^{-1}$) but the smallest annual value (0.04 g N $m^{-2}yr^{-1}$) among three C-N schemes. For the N immobilization fluxes, SM3 simulated the largest daily variation (0.0013 g N $m^{-2}d^{-1}$) and SM1 showed the largest annual mean value (1.15 g N $m^{-2}yr^{-1}$). The dynamics of soil mineral N in SM2 and SM3 displayed the similar patterns on the daily and annual dynamics.

Compared with the TECO-C model, the three C-N coupling schemes introduced significant signs of N limitation on forest growth at the steady state but with varying strength (Fig 4). Specifically, the three N schemes resulted in significant reductions in GPP (10%, 10% and 12% for SM1, SM2 and SM3, respectively) compared to the C-only TECO model. Similar response patterns were also found on NPP, ecosystem respiration, and heterotrophic respiration. Among

Geosci. Model Dev. Discuss., https://doi.org/10.5194/gmd-2018-41
Manuscript under review for journal Geosci. Model Dev.
Discussion started: 15 March 2018

the three schemes, SM3 had the strongest effect (45%, 12% and 45% reduction for NPP, ecosystem respiration, and heterotrophic respiration, respectively), SM2 had the weakest effect (15%, 8% and 13%, respectively) and the effect in SM1 was moderate (29%, 10% and 29%, respectively). However, both the SM1 and SM2 schemes increased the autotrophic respiration (R-auto) by 12% and 27%, respectively, and SM2 scheme increased the NEE by 32%. Due to the NSC pool of TECO model, NEE were positive in all the experiments at the steady state (Weng and Luo, 2008). The NPP and plant N uptake (PNU) joint determine the N use efficiency (NUE). The divergent effects of three C-N schemes on NPP and PNU lead to different NUE (Fig. 5). SM1 had the highest NUE (159.1 g C g^{-1} N), mainly resulting from its lowest PNU. In contrast, SM3 had the lowest NUE (67.3 g C g^{-1} N) as a result of its smallest NPP.

3.2 Simulation of C storage capacity

The ecosystem C storage capacity differed greatly among the three C-N coupling schemes as well as with the C-only version of TECO model (Fig. 6). The C-only version had the largest C storage capacity (19.5 Kg C m^{-2}) among the four simulations, resulting from its highest NPP (879.9 g C m^{-2} yr^{-1}). The C storage capacity in SM1 (15.1 Kg C m^{-2}) was close to that in SM2 (13.7 Kg C m^{-2}). The SM3 had the lowest C storage capacity (8.9 Kg C m^{-2}) among the four simulations as a result of its smallest NPP (483.9 g C m^{-2} yr^{-1}) and relative short MRT (18.6 years). By comparison with the C-only version, the three C-N schemes all induced different reductions on NPP (-29%, -15% and -45% for SM1, SM2, SM3, respectively) and further reduced their ecosystem C storage capacity. For the MRT, the three C-N schemes exhibited contrasting effects between SM1 (+9%) and another two schemes (i.e., -16.9% in SM2 and -16.7% in SM3) compared with the C-only TECO model.

3.3. Ecosystem C residence time

Ecosystem C residence time (τ_E) is collectively determined by baseline residence time, N scalar and environmental scalar as shown in Eqn (30). Specifically, differences in τ_E among three C-N coupling schemes and C-only TECO model are determined by baseline residence time and the effects of N scalar on eight plant C pools (Fig. 7). For example, SM1 had the longest τ_E because the N scalar had very strong control on passive SOM. The baseline residence time were further determined by the C allocation pattern (Fig. 8). Overall, compared with C-only version, the

additional N processes enhanced the partitioning coefficient of NPP to roots (33%, 82% and 53%, respectively for SM1, SM2 and SM3), while it decreased the partitioning coefficient to wood (-25%, -45% and -34%, respectively). Furthermore, the decreased partitioning coefficient to wood (b2) regulated the variations of the baseline residence time of wood, structural litter, slow and passive SOM. However, the increased partitioning coefficient to roots (b3) determined the variations of the baseline residence time of root and metabolic litter.

3.4. Sensitivity of N processes to NPP and MRT

For either NPP or MRT, the N processes had different sensitivities among the three C-N schemes of TECO model (Fig. 9). For NPP, plant C:N ratio had the highest sensitivities in both SM1 (0.32) and SM2 (0.53). However, plant N uptake in SM3 had the highest sensitivity (0.87) for NPP. For MRT, competition between plants and microbes, down-regulation photosynthesis and plant C:N had the highest sensitivities in SM1 (0.27), SM2(0.19) and SM3 (0.56), respectively.

4. Discussions

4.1 Underlying N processes and plant production

Gross or net primary production (i.e., NPP or GPP) is regulated by the amount of N available for growth through the N demand, which is set by the relative proportion of biomass growth in the different plant components and their C:N stoichiometry (Zaehle et al., 2014; Thomas et al., 2015). The limitation of equilibrium N on plant production reflects the effects from multiple processes of the C-N interaction, mainly including down-regulation of photosynthetic capacity (DRP) by N availability, the ecosystem's balance of N inputs and losses (net ecosystem N exchange, NNE), plant N uptake (PNU), soil N mineralization (SNM), and the C:N stoichiometry of vegetation and soils. However, due to a lack of consensus on the nature of the mechanisms, the representation of these processes varies greatly among models (Zaehle et al., 2014).

There are two common alternative assumptions of the DRP that have been implemented in models: (1) the change in photosynthetic capacity is directly associated with the magnitude of plant available N (e.g., SM2), and (2) N limitation is associated with foliage N, which feeds back to limit photosynthetic capacity (e.g., SM1 and SM3). Our results showed that both assumptions had significant limitations with similar effects on GPP (Fig.3). The probable reason is that the

Geosci. Model Dev. Discuss., https://doi.org/10.5194/gmd-2018-41
Manuscript under review for journal Geosci. Model Dev.
Discussion started: 15 March 2018

TECO model calculates photosynthesis by light availability vs. carboxylation rate based on the Farquhar model (Farquhar et al., 1980). The effects of N stress under TECO framework, either associated with plant available N or associated with foliage N concentration, are estimated according to limiting factors of photosynthetic biochemistry (the maximum rate of carboxylation, V_{cmax}, and the maximum rate of electron transport at saturating irradiance, V_{jmax}).

At or near the steady state, NNE is driven by the processes of N input via deposition and fixation and N loss via leaching and volatilization stoichiometry (Zaehle et al., 2014; Thomas et al., 2015). Previous studies have stated that analyzing the steady-state condition is useful to understand N effects because the balance between external N sources and N losses determine whether an ecosystem is N limited (Rastetter et al., 1997; Menge et al., 2009; Thomas et al., 2015). In this study, divergent NPP responses among three schemes might partly result from their different representations of BNF. For example, SM2 and SM3 simulated BNF explicitly, which used modified empirical relationships to calculate BNF based on evapotranspiration (ET) and NPP, respectively. These phenomenological relationships generally captured biogeographical observations of higher rates of BNF in humid environments with high solar radiation (Wieder et al., 2015). However, the highest response of NPP in only ET-driven BNF (i.e., SM3) may illustrate that not only energetic but also C costs of 'fixing' atmospheric di-N (N_2) into a biologically usable form (NH_3) broadly affect NPP (Gutschick 1981, Rastetter et al., 2001). This was because SM3 considered C investments in BNF while SM2 did not. On the other hand, SM1 applied a different strategy, which represents BNF as a complement to the plant N uptake in terms of C investment, leading to the highest plant NUE but the lowest response of BNF to NPP. Another driving factor of NNE is the N loss, which depends on the rate of leaching and volatilization. Using the same formulation as proportional to the size of soil mineral N pool among three schemes, the divergent annual mean magnitude of N leaching was more correlated to soil mineral N.

The processes of PNU and net N mineralization determine how N moves through the plant-soil system, thereby triggering N limitation on plant growth. However, to our knowledge, exploring those processes exactly in models is limited by inadequate representation of above- and below-ground interactions that control the patterns of N allocation and whole-plant stoichiometry (Zaehle et al., 2014; Thomas et al., 2015). Plant tissue, litter, and SOM are the primary sinks of N in terrestrial ecosystems, while N in these forms is not directly available for

Geosci. Model Dev. Discuss., https://doi.org/10.5194/gmd-2018-41
Manuscript under review for journal Geosci. Model Dev.
Discussion started: 15 March 2018

PNU, leading to an increase in N demand due to plant growth. On the other hand, these N must turn over to become available for plant growth. Therefore, the time for N to stay in these unavailable pools controls the transactional delay between the incorporation of N into plant unavailable pool and becomes available for plant uptake. In this way, the residence time of N in SOM appears to be an important factor for governing plant growth (see next section). In the present study, SM1 had the highest NUE from the combined effects of PNU based on C investment strategy (as described above) and flexible tissue C:N ratio. N stress increased tissue C:N ratio, leading to a high microbial N immobilization and then a lower net N mineralization, which allowed plant cell construction with a lower N requirement. The inclusion of flexible C:N stoichiometry (i.e., PS&SS) appeared to be an important feature allowing models to capture the ecosystem response to climate variability through adjusting the C:N ratio of nonphotosynthetic tissues or the whole-plant allocation among tissues with different C:N ratios (Zaehle & Friend, 2010). However, it is unclear whether those regulatory mechanisms exist in reality. Further modelling approaches need more reliable framework to predict stoichiometric flexibility.

4.2 Ecosystem N status and C residence time

Ecosystem N status in models, including plant-available and unavailable N forms, is set by N inputs from N fixation and N deposition, N losses from leaching and denitrification, and N gain from the turnover of litter and SOM through tissue senescence and decomposition. As noted above, external N cycle (i.e., N inputs and N losses) couples the N processes within the plant-litter-SOM system, being mainly associated with the limitation of plant production. The effects of ecosystem N status on C mean residence time (MRT), however, has been much less studied than N limitation on productivity of plants and soil organisms, largely because these effects involve various impacts on C transfer among pools and release from each pool via decomposition and respiration (Thompson & Randerson, 1999; Xia et al., 2013). Therefore, the different impacts of ecosystem N status induce oscillating N limitation on MRT due to the inherently different assumptions of C-N interactions among three C-N coupling schemes.

At the steady state, the different effects of N status on changes in modelled MRT can be attributed to: the different rate of soil N mineralization dependent on the total amount of N in SOM and its turnover time, immobilization based on the competition strategy between plants and microbes and their stoichiometry, and different deployment of reabsorbed N . The traceability

Geosci. Model Dev. Discuss., https://doi.org/10.5194/gmd-2018-41
Manuscript under review for journal Geosci. Model Dev.
Discussion started: 15 March 2018

framework in this study can trace those different effects into three components (i.e., climate forcing, N scalar and baseline MRT) based on three alternative C-N coupling schemes under the TECO model framework. Since the forcing data are identical, we assumed the same effects for this component in all four experiments, which is thus not discussed further in this section.

In our study, the N scalar was based on the dynamics of C:N ratios (Eqn. 33). Therefore, N scalar had no effect on MRT in SM2, resulting from the assumption of fixed C:N ratio in all C pools (Fig. 6c). In both SM1 and SM3, however, the N scalar had large effects on the SOM pool, which is probably related to different mechanisms. Specifically, N scalar in the SM1 had the contrasting effects on MRT of fast and passive SOM pools (i.e., negative vs. positive, respectively), which may largely be attributed to the plant and microbe competition strategy combining with a much larger passive SOM pool in TECO-CN2.0 model (Du et al., 2017; Zhu et al., 2017). Under N stress, the competition between plants and microbes is expected to be intensified, resulting in increasing C:N ratio of nonphotosynthetic tissues (e.g., wood and root) and the total C:N ratio. This effectively prevents N limitation of cell construction and corresponds to an increase in whole-plant NUE (Thomas et al., 2015). In this case, higher C:N ratio in those tissues lowers structural litter quality, leading to soil microbes to immobilize more N to maintain their stoichiometric balance (Hu et al., 2001; Manzoni et al., 2010). However, in the SM3, increased respiration acted as a mechanism to remove the excess accumulated C, which is a stoichiometry-based implementation to prevent the accumulation of labile C under N stress (Zaehle & Friend, 2010; Thomas et al., 2015). This mechanism promotes absorption and respiration of the faster turnover pools (fast and slow SOM pools), leading to decrease in MRT in these two pools.

In the traceability framework, the baseline MRT is determined by the potential decomposition rates of C pools (C matrix), coefficients of C partitioning of NPP (B vector), and transfer coefficients between C pools (*A* matrix, Eqn. [29]. Xia et al., 2013). The matrices *A* and *C* are preset in the TECO model according to vegetation characteristics and soil textures (Weng and Luo., 2008). Therefore, the notable spread in baseline MRT across the C-N schemes was induced by the *B* vector, which was modified by different N-limitation assumptions. Conceptually, in order to meet the N demand, plants adjust NPP allocation to N absorption tissues (e.g., roots). In this study, three schemes all had similar trends of adjusting allocation C from wood to roots (Fig. 7), but with different mechanisms. For both SM1 and SM3, increased root C allocation was

mainly driven by N uptake capacity, which is associated with plant competitiveness in SM1 and the respiration of excess labile C in SM3, respectively. However, for SM2, increasing root C allocation may occur in spin-up stage from plant adjustment to whole-plant allocation among tissues to fit fixed C:N ratio.

5. Conclusions

The C-N coupling has been represented in ecosystem and land surface models with different schemes, generating great uncertainties in model predictions. The most striking difference among terrestrial C-N coupling models occurs with the degree of flexibility of C:N ratio in vegetation and soils, plant N uptake strategies, pathways of N import, and the representations of the competition between plants and microbes for soil mineral N. In this study, we evaluated alternative representations of C-N interactions and their impacts on C cycle using the TECO model framework. Our traceability analysis showed that different representations of C-N coupling processes lead to divergent effects on both plant production and C residence time, and thus the ecosystem C storage capacity. The plant production are mainly affected by the different assumptions on net ecosystem N exchange, plant N uptake, net N mineralization, and the C:N ratio of vegetation and soil. In comparison, the alternative representations of the plant and microbe competition strategy, combining with the flexible C:N ratio in vegetation and soils, led to a notable spread effects on C residence time. Identifying the representations of main C-N processes under different schemes can help us to improve the N-limitation assumptions employed in terrestrial ecosystem models and forecasting future C sink dynamic in response to climate change.

Code availability. The code for TECO-CN2.0 and the three C-N coupling schemes is available at https://github.com/zgdu/TECO-CN-2.0-new.

Data availability. The data for this paper are available upon request to the corresponding author.

Competing interests. The authors declare that they have no conflict of interest.

Acknowledgements

This work was financially supported by the National Key R&D Program of China (2017YFA06046), the National Natural Science Foundation of China (31770559, 31722009), National 1000 Young Talents Program of China, and the Fundamental Research Funds for Central Universities. Zhenggang Du also thanks the China Scholarship Council (201606140130) for scholarship support.

Geosci. Model Dev. Discuss., https://doi.org/10.5194/gmd-2018-41
Manuscript under review for journal Geosci. Model Dev.
Discussion started: 15 March 2018

Geoscientific Model Development Discussions

Figure legends

Figure 1. Schematic diagram of the terrestrial ecosystem carbon (C) and nitrogen (N) coupling model (TECO-CN2.0). (A) Canopy module, (B) Plant growth module, (C) Soil water dynamics module, (D) Soil carbon-nitrogen coupling module. Rectangles represent the carbon and nitrogen pools. R_a, autotrophic respiration. R_h, heterotrophic respiration. Retr., re-translocation. NSC, nonstructural carbohydrate. MNP, mineral N in plant tissues. SOM, soil organic matter.

Figure 2. Schematic diagram illustrating the major carbon (C) and nitrogen (N) flows and stores in a terrestrial ecosystem. Light-blue arrows indicate C-cycle processes and red arrows show N-cycle processes.[1,2,3] alternative assumptions of N processes represent in scheme 1, 2 and 3, respectively. Met./Str. Litter, metabolic and/or structural litters; SOM, soil organic matter.

Figure 3. Simulated nitrogen fluxes and soil mineral nitrogen from three carbon-nitrogen coupling schemes (SM1, SM2 and SM3) in TECO-CN model for 1996 to 2007 at Duke Forest.

Figure 4. Simulated annual (a-f) and mean (g-l) carbon fluxes from carbon-only version and carbon-nitrogen coupled with three schemes (SM1, SM2 and SM3) of TECO model for 1996 to 2007 at Duke Forest. GPP, gross primary productivity; NPP, net primary productivity; NEE, net ecosystem exchange of CO_2; R-eco, ecosystem respiration; R-heter, heterotrophic respiration; R-auto, autotrophic respiration.

Figure 5. The nitrogen use efficiency (NUE) in three C-N schemes of TECO model (SM1, SM2 and SM3).

Figure 6. Simulation of annual ecosystem carbon storage capacity for 1996 to 2006 at Duke Forest by carbon in flux (NPP, x axis) and ecosystem residence time (τ_E, y axis) in TECO model framework with three carbon-nitrogen coupling schemes (SM1, SM2 and SM3) and in TECO C-only model (C). Inset (a), ecosystem carbon residence time (τ_E) in SM1, SM2, SM3 and C-only model; inset (b), mean ecosystem carbon storage simulated among SM1, SM2, SM3 and C-only model; inset (c), relative change of NPP and ecosystem residence time simulated among three schemes compared with in C-only model.

Figure 7. Determination of carbon-pool residence times based on traceability framework in TECO C-N model with three C-N coupling schemes (SM1, SM2 and SM3) and TECO C-only model (C). Panel (a), baseline residence time; panel (b), mean residence time, and panel (c), nitrogen scalar.

Figure 8. Coefficients of partitioning of NPP to nonstructural C (NSC), root, woody and leaf in C-only model (C) and C-N coupling model with three schemes (SM1, SM2 and SM3).

Figure 9. The sensitivity of nitrogen processes to NPP (panel a) and ecosystem residence time (τ_E, panel b) among three carbon-nitrogen coupling schemes (SM1, SM2 and SM3). DRP, down-regulation photosynthesis; PS, plant tissue C:N ratio; PNU, plant N uptake; PMC: plant and microbe competition; BNF, biological N fixation; RtrN, re-tranlocation N; SS, soil pool C:N ratio.

Reference

Cleveland, C.C., Townsend, A.R., Schimel, D.S., Fisher, H., Howarth, R.W., Hedin, L.O., Perakis, S.S., Latty, E.F., Von Fischer, J.C., Elseroad, A. and Wasson, M.F., 1999. Global patterns of terrestrial biological nitrogen (N2) fixation in natural ecosystems. Global biogeochemical cycles, 13(2), pp.623-645.

Cleveland, C.C., Houlton, B.Z., Smith, W.K., Marklein, A.R., Reed, S.C., Parton, W., Del Grosso, S.J. and Running, S.W., 2013. Patterns of new versus recycled primary production in the terrestrial biosphere. Proceedings of the National Academy of Sciences, 110(31), pp.12733-12737.

Denison, R.F. and Loomis, R.S., 1989. An integrative physiological model of alfalfa growth and development. Publication/University of California, Division of Agriculture and Natural Resources (USA).

Du, Z., Zhou, X., Shao, J., Yu, G., Wang, H., Zhai, D., Xia, J., Luo, Y. (2017). Quantifying uncertainties from additional nitrogen data and processes in a terrestrial ecosystem model with Bayesian probabilistic inversion. Journal of Advances in Modeling Earth Systems, 9(1), 548-565.

Farquhar GD, Caemmerer SV, Berry JA. 1980. A biochemical model of photosynthetic CO_2 assimilation in leaves of C3 species. Planta, 149, 78–90.

Finzi, A.C., Norby, R.J., Calfapietra, C., Gallet-Budynek, A., Gielen, B., Holmes, W.E., Hoosbeek, M.R., Iversen, C.M., Jackson, R.B., Kubiske, M.E. and Ledford, J., 2007. Increases in nitrogen uptake rather than nitrogen-use efficiency support higher rates of temperate forest productivity under elevated CO2. Proceedings of the National Academy of Sciences, 104(35), pp.14014-14019.

García - Palacios, P., Maestre, F.T., Kattge, J. and Wall, D.H., 2013. Climate and litter quality differently modulate the effects of soil fauna on litter decomposition across biomes. Ecology letters, 16(8), pp.1045-1053.

Gerber S, Hedin LO, Oppenheimer M, Pacala SW, Shevliakova E (2010) Nitrogen cycling and feedbacks in a global dynamic land model. Global Biogeochemical Cycles, 24, GB1001.

GutschickVP (1981) Evolved strategies of nitrogen fixation in plants Am. Naturalist 118 607–37

Hendrey, G.R., Ellsworth, D.S., Lewin, K.F. and Nagy, J., 1999. A free‐air enrichment system for exposing tall forest vegetation to elevated atmospheric CO2. Global Change Biology, 5(3), pp.293-309.

Houlton, B. Z., Y. P. Wang, P. M. Vitousek, and C. B. Field (2008), A unifying framework for dinitrogen fixation in the terrestrial biosphere, Nature, 454, 327–330, doi:10.1038/nature07028.

Lichter J, Billings SA, Ziegler SE, Gaindh D, Ryals R, Finzi AC, Jackson RB, Stemmler EA, Schlesinger WH. 2008. Soil carbon sequestration in a pine forest after 9 years of atmospheric CO2 enrichment. Global Change Biology 14: 2910–2922.

Luo, Y., Meyerhoff, P.A. and Loomis, R.S., 1995. Seasonal patterns and vertical distributions of fine roots of alfalfa (Medicago sativa L.). Field Crops Research, 40(2), pp.119-127.

Luo Y, Reynolds JF (1999) Validity of extrapolating field CO2 experiments to predict carbon sequestration in natural ecosystems. Ecology, 80, 1568-1583.

Luo, Y, LW. White, JG. Canadell, EH. DeLucia, DS. Ellsworth, A Finzi, J Lichter, and WH Schlesinger (2003). Sustainability of terrestrial carbon sequestration: a case study in Duke Forest with inversion approach. Global biogeochemical cycles, 17(1).

Luo, Y., Su, B.O., Currie, W.S., Dukes, J.S., Finzi, A., Hartwig, U., Hungate, B., McMurtrie, R.E., Oren, R.A.M., Parton, W.J. and Pataki, D.E., 2004. Progressive nitrogen limitation of ecosystem responses to rising atmospheric carbon dioxide. AIBS Bulletin, 54(8), pp.731-739.

Luo, Y, and E Weng. 2011. Dynamic disequilibrium of the terrestrial carbon cycle under global change. Trends in Ecology & Evolution 26(2): 96-104.

Luo Y, Keenan T F, Smith M. Predictability of the terrestrial carbon cycle. 2015. Global change biology, 21(5): 1737-1751.

McCarthy HR, Oren R, Johnsen KH, Gallet-Budynek A, Pritchard SG, Cook CW, LaDeau SL, Jackson RB, Finzi AC. 2010. Re-assessment of plant carbon dynamics at the Duke free-air CO2 enrichment site: interactions of atmospheric [CO2] with nitrogen and water vailability over stand development. New Phytologist 185: 514–528.

McMurtrie RE, Iversen CM, Dewar RC, Medlyn BE, Nasholm T, Pepper DA, Norby RJ. 2012. Plant root distributions and nitrogen uptake predicted by a hypothesis of optimal root foraging. Ecology and Evolution, 2, 1235-1250.

634 Melillo JM, McGuire AD, Kicklighter DW, Moore B III, Vorosmarty CJ, Schloss A (1993)
635 Global climate change and terrestrial net primary production. Nature, 363, 234–240.
636 Menge DNL, Pacala SW, Hedin LO. 2009. Emergence and maintenance of nutrient limitation
637 over multiple timescales in terrestrial ecosystems. The American Naturalist, 173, 164–175.
638 van Oijen, M., and P. Levy. 2004. Nitrogen metabolism and plant adaptation to the environment:
639 The scope for process-based modeling, in Nitrogen Acquisition and Assimilation in Higher
640 Plants, Plant Ecophysiol. Ser., vol. 3, edited by S. Amaˆncio and I. Stulen, pp. 133– 147,
641 Kluwer Acad., Dordrecht, Netherlands.
642 Parton WJ, Hanson PJ, Swanston C, Torn M, Trumbore SE, Riley W, Kelly R. 2010. ForCent
643 model development and testing using the Enriched Background Isotope Study experiment.
644 Journal of Geophysical Research 115: G04001.
645 Rastetter EB, Agren GI, Shaver GR. 1997. Responses of N-limited ecosystems to increased CO2:
646 a balanced-nutrition, coupled-element-cycles model. Ecological Applications, 7: 444–460.
647 Rastetter EB, Vitousek PM, Field C, Shaver G, Herbert D, Agren GI (2001) Resource
648 optimization and symbiotic nitrogen fixation. Ecosystems, 4, 369–388.
649 Shevliakova, E., Pacala, S.W., Malyshev, S., Hurtt, G.C., Milly, P.C.D., Caspersen, J.P.,
650 Sentman, L.T., Fisk, J.P., Wirth, C. and Crevoisier, C., 2009. Carbon cycling under 300 years
651 of land use change: Importance of the secondary vegetation sink. Global Biogeochemical
652 Cycles, 23(2).
653 Sprugel, D. G., M. G. Ryan, J. R. Brooks, K. A. Vogt, and T. A. Martin (1996), Respiration from
654 the organ level to the stand, in Resource Physiology of Conifers, edited by K. Smith and T. M.
655 Hinckley, pp. 255–299, Academic, San Diego, Calif.
656 Thomas, R.Q., Zaehle, S., Templer, P.H. and Goodale, C.L., 2013. Global patterns of nitrogen
657 limitation: confronting two global biogeochemical models with observations. Global change
658 biology, 19(10), pp.2986-2998.
659 Thomas, R. Quinn, E. N. Brookshire, and Stefan Gerber. Nitrogen limitation on land: how can it
660 occur in Earth system models?. Global change biology, 2015, 21(5): 1777-1793.
661 Thompson MV, Randerson JT. Impulse response functions of terrestrial carbon cycle models:
662 method and application. Global Change Biology, 1999, 5, 371–394.

663 Thornton P E, Lamarque J F, Rosenbloom N A, et al. Influence of carbon‐nitrogen cycle
664 coupling on land model response to CO2 fertilization and climate variability. Global
665 biogeochemical cycles, 2007, 21(4).
666 Vitousek P M, Howarth R W. Nitrogen limitation on land and in the sea: how can it occur?.
667 Biogeochemistry, 1991, 13(2): 87-115.
668 Wang S, Grant RF, Verseghy DL, Black TA. 2001. Modelling plant carbon and nitrogen
669 dynamics of a boreal aspen forest in CLASS – the Canadian Land Surface Scheme.
670 Ecological Modelling 142: 135–154.
671 Wang YP, Law RM, Pak B., 2010. A global model of carbon, nitrogen and phosphorus cycles for
672 the terrestrial biosphere. Biogeosciences, 7, 2261–2282.
673 Weng E, Luo Y., 2008. Soil hydrological properties regulate grassland ecosystem responses to
674 multifactor global change: A modeling analysis. Journal of Geophysical Research:
675 Biogeosciences, 113(G3).
676 Wieder, W.R., Cleveland, C.C., Smith, W.K. and Todd-Brown, K., 2015. Future productivity
677 and carbon storage limited by terrestrial nutrient availability. Nature Geoscience, 8(6), p.441.
678 Xia, J.Y., Luo, Y.Q., Wang, Y.P., Weng, E.S. and Hararuk, O., 2012. A semi-analytical solution
679 to accelerate spin-up of a coupled carbon and nitrogen land model to steady state.
680 Geoscientific Model Development, 5(5), pp.1259-1271.
681 Xia, J., Luo, Y., Wang, Y.P. and Hararuk, O., 2013. Traceable components of terrestrial carbon
682 storage capacity in biogeochemical models. Global Change Biology, 19(7), pp.2104-2116.
683 Zaehle, S. and Friend, A.D., 2010. Carbon and nitrogen cycle dynamics in the O‐CN land
684 surface model: 1. Model description, site‐scale evaluation, and sensitivity to parameter
685 estimates. Global Biogeochemical Cycles, 24(1).

686 Zaehle, S. and Dalmonech, D., 2011. Carbon–nitrogen interactions on land at global scales:
687 current understanding in modelling climate biosphere feedbacks. Current Opinion in
688 Environmental Sustainability, 3(5), pp.311-320.

689 Zaehle, S., Medlyn, B.E., De Kauwe, M.G., Walker, A.P., Dietze, M.C., Hickler, T., Luo, Y.,
690 Wang, Y.P., El‐Masri, B., Thornton, P. and Jain, A., 2014. Evaluation of 11 terrestrial
691 carbon–nitrogen cycle models against observations from two temperate Free‐Air CO2
692 Enrichment studies. New Phytologist, 202(3), pp.803-822.

693 Zhou, L., Zhou, X., Zhang, B., Lu, M., Luo, Y., Liu, L. and Li, B., 2014. Different responses of
694 soil respiration and its components to nitrogen addition among biomes: a meta‐analysis.
695 Global change biology, 20(7), pp.2332-2343.

696 Zhu, Q., Riley, W. J., & Tang, J. (2017). A new theory of plant–microbe nutrient competition
697 resolves inconsistencies between observations and model predictions. Ecological Applications,
698 27(3), 875-886.

699

Geosci. Model Dev. Discuss., https://doi.org/10.5194/gmd-2018-41
Manuscript under review for journal Geosci. Model Dev.
Discussion started: 15 March 2018

Geoscientific Model Development Discussions

700 **Table1.** Summary of the nitrogen-carbon coupling schemes used and the representation of key
701 processes in the carbon-nitrogen cycle.

	SM1 (TECO-CN2.0)[a]	**SM2 (CLM4.5)**[b,c]	**SM3 (O-CN)**[d,e]
Photosynthesis down regulation by N availability (DRP)	Based on the comparison between plant N demand and actual supply	Based on the available soil mineral N relative to the N demanded to allocate photosynthate to tissue	Based on foliage N concentration, which varies with N deficiency
Plant tissue stoichiometry (PS)	Flexible plant C:N ratio	Fixed plant C:N ratio	Flexible plant C:N ratio
Plant N uptake (PNU)	Based on fine root biomass, soil mineral N and N demand of plant. Plants itself choose the strategy between uptake from soil mineral N and fix N_2 by comparing C investment	Based on N required to allocate NPP to tissue. Plants uptake N for free	Combining active and passive uptake of mineral N based on fine root C, soil mineral N, plant transpiration flux, increases with increased plant N demand
N competition between plants and microbes (PMC)	Microbes have first access to soil mineral N	Based on demand by both microbial immobilization and plant N uptake	Microbes have first access to soil mineral N, the competitive strength of plants increases under nutrient stress
Biological N fixation (BNF)	Based on the nitrogen demand of plants and maximum N fixing ratio considering nutrient concentration	$f(NPP)$	$f(ET)$
Deployment of re-translocated N (RtrN)	Fixed fraction of litter	Based on available N in the tissue and the previous year's annual sum of plant N demand	Fixed fraction of dying leaf and root tissue
Soil organic matter stoichiometry (SS)	Flexible soil C:N ratio	Fixed soil C:N ratio	Flexible soil C:N ratio
N leaching	Function of soil mineral N pool and runoff	Function of soil mineral N pool and runoff	Function of soil mineral N and runoff

702 [a]See this study; [b]Thornton et al. (2007), [c]Thornton et al. (2009); [d] Zaehle &Friend (2010),
703 [e]Zaehle et al. (2011).

704 C, carbon; N, nitrogen; NPP, net primary productivity; ET, evapotranspiration.

Geosci. Model Dev. Discuss., https://doi.org/10.5194/gmd-2018-41
Manuscript under review for journal Geosci. Model Dev.
Discussion started: 15 March 2018

705 **Figure 1. TECO-CN 2.0**

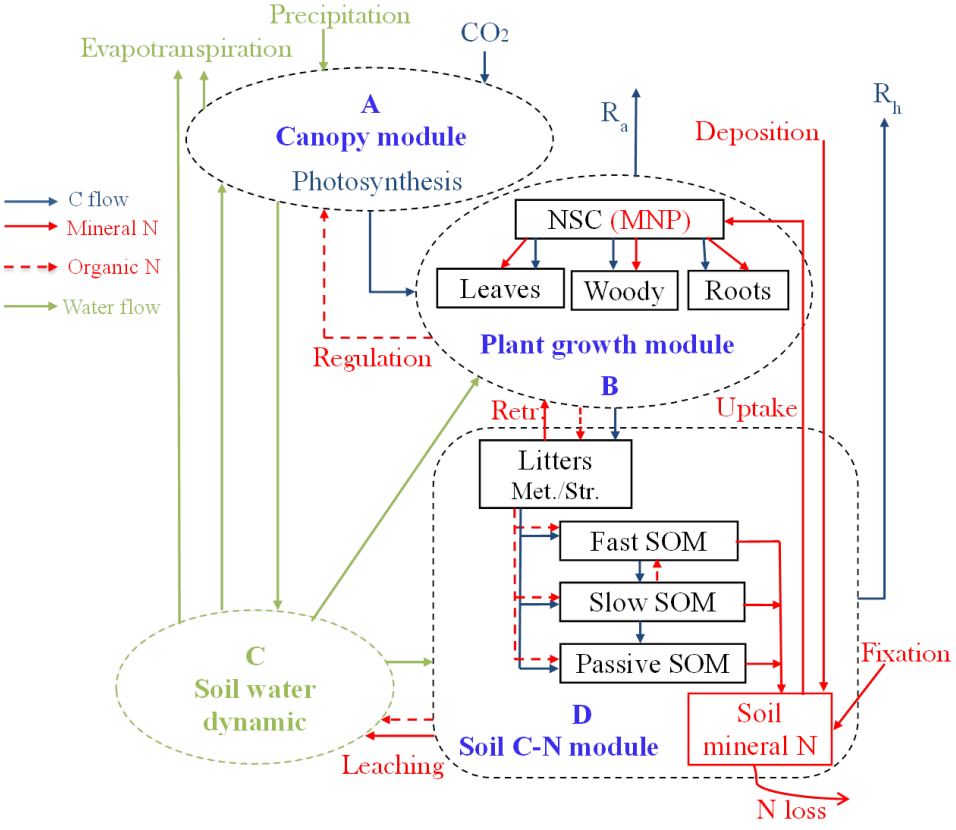

706

707 **Figure 1.** Schematic diagram of the terrestrial ecosystem carbon (C) and nitrogen (N) coupling
708 model (TECO-CN2.0). (A) Canopy module, (B) Plant growth module, (C) Soil water dynamics
709 module, (D) Soil carbon-nitrogen coupling module. Rectangles represent the carbon and nitrogen
710 pools. R_a, autotrophic respiration. R_h, heterotrophic respiration. Retr., re-translocation. NSC,
711 nonstructural carbohydrate. MNP, mineral N in plant tissues. SOM, soil organic matter.
712

Geosci. Model Dev. Discuss., https://doi.org/10.5194/gmd-2018-41
Manuscript under review for journal Geosci. Model Dev.
Discussion started: 15 March 2018

Geoscientific Model Development Discussions

713 **Figure 2**

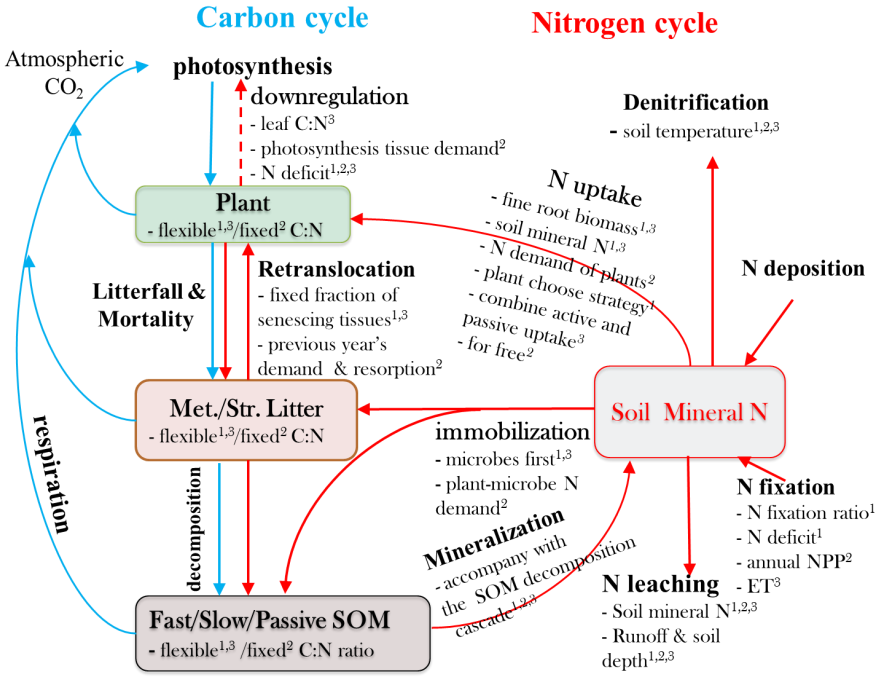

714

715

716 **Figure 2.** Schematic diagram illustrating the major carbon (C) and nitrogen (N) flows and stores
717 in a terrestrial ecosystem. Light-blue arrows indicate C-cycle processes and red arrows show N-
718 cycle processes.[1,2,3] alternative assumptions of N processes represent in scheme 1, 2 and 3,
719 respectively. Met./Str. Litter, metabolic and/or structural litters; SOM, soil organic matter.

720

Geosci. Model Dev. Discuss., https://doi.org/10.5194/gmd-2018-41
Manuscript under review for journal Geosci. Model Dev.
Discussion started: 15 March 2018

721 **Figure 3**

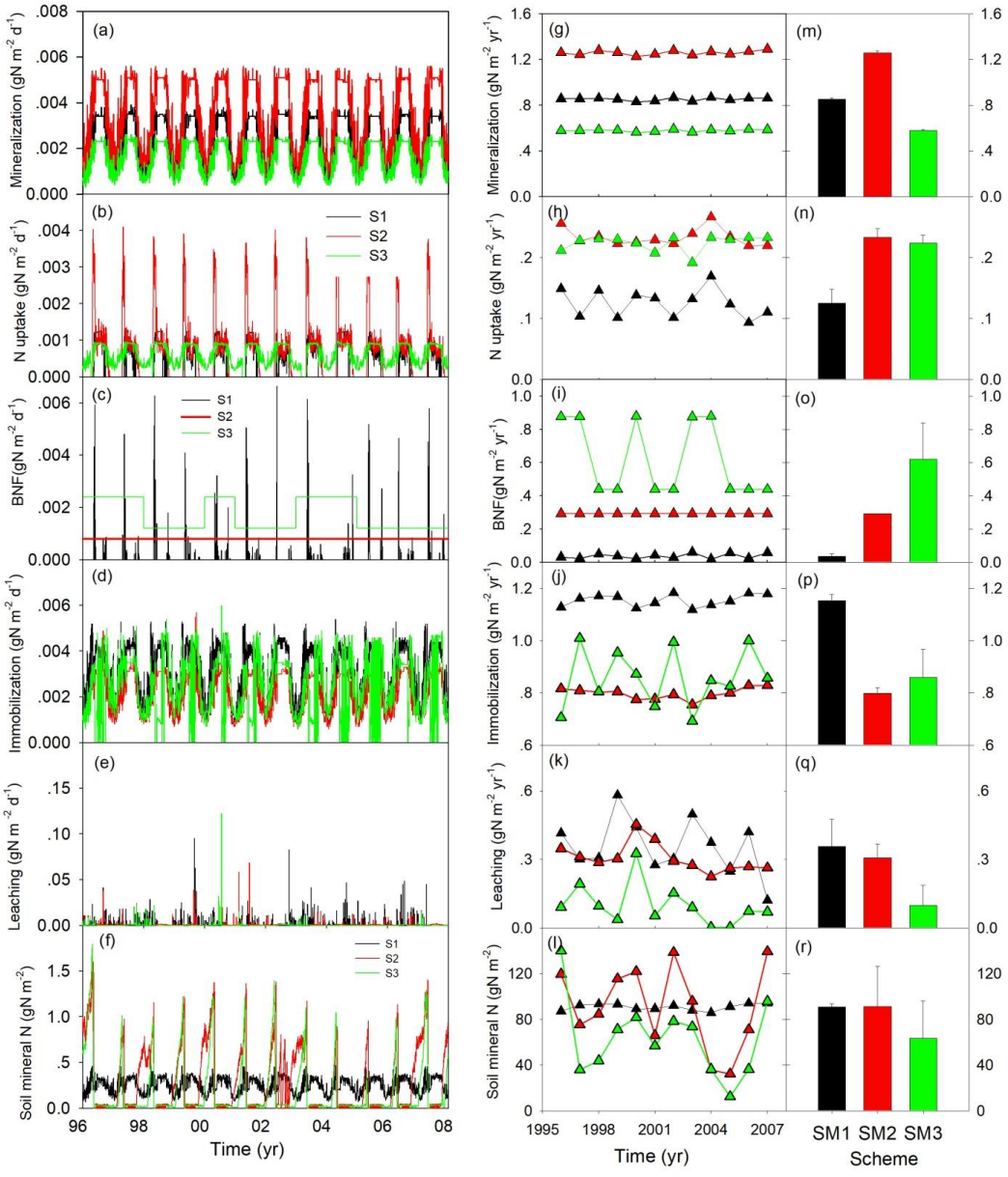

722

723 **Figure 3.** Simulated nitrogen fluxes and soil mineral nitrogen from three carbon-nitrogen
724 coupling schemes (SM1, SM2 and SM3) in TECO-CN model for 1996 to 2007 at Duke Forest.

725

Geosci. Model Dev. Discuss., https://doi.org/10.5194/gmd-2018-41
Manuscript under review for journal Geosci. Model Dev.
Discussion started: 15 March 2018

726 **Figure 4**

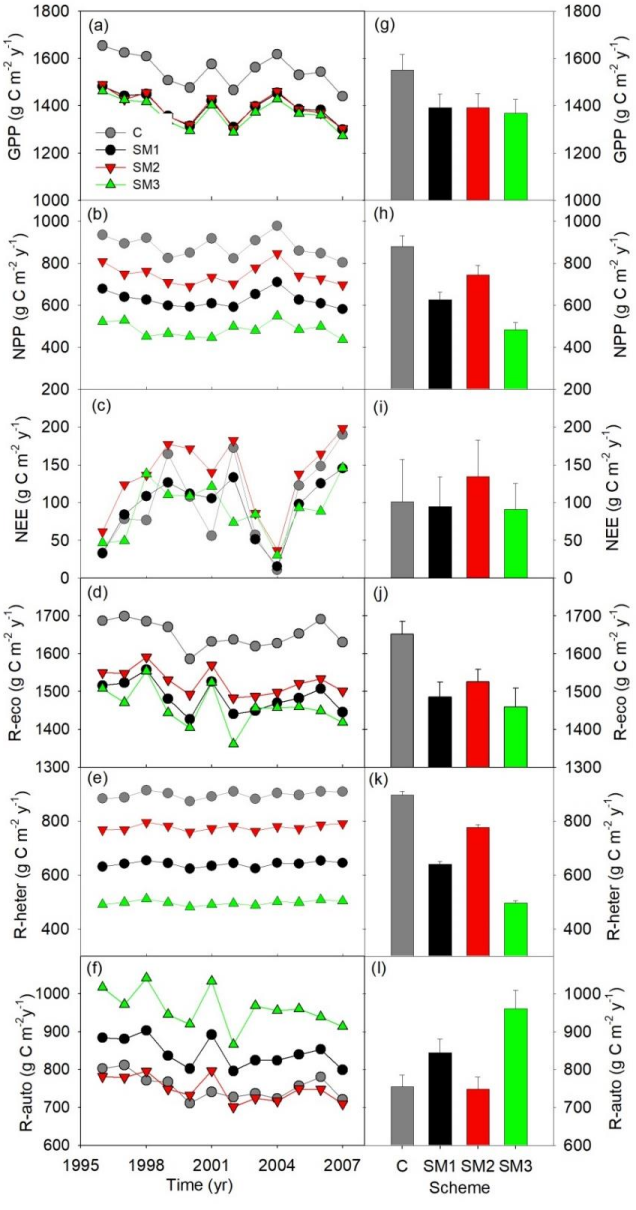

727

728 **Figure 4.** Simulated annual (a-f) and mean (g-l) carbon fluxes from carbon-only version and
729 carbon-nitrogen coupled with three schemes (SM1, SM2 and SM3) of TECO model for 1996 to
730 2007 at Duke Forest. GPP, gross primary productivity; NPP, net primary productivity; NEE, net
731 ecosystem exchange of CO_2; R-eco, ecosystem respiration; R-heter, heterotrophic respiration; R-
732 auto, autotrophic respiration.

Geosci. Model Dev. Discuss., https://doi.org/10.5194/gmd-2018-41
Manuscript under review for journal Geosci. Model Dev.
Discussion started: 15 March 2018

733 **Figure 5**

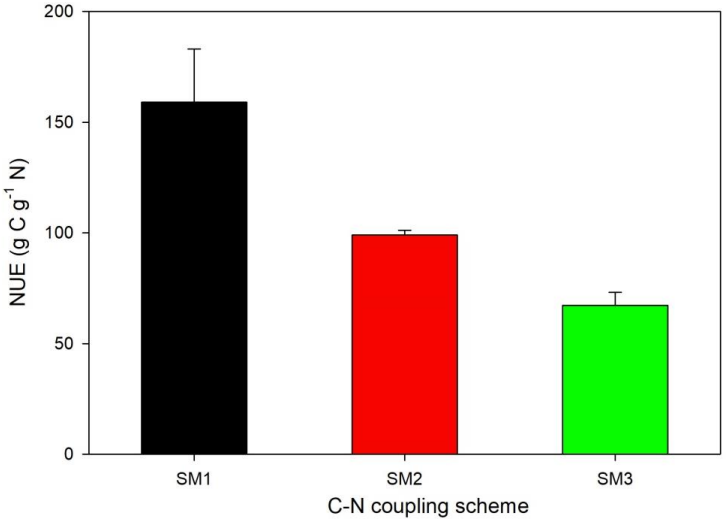

734

735 **Figure 5.** The nitrogen use efficiency (NUE) in three C-N schemes of TECO model (SM1, SM2
736 and SM3).

737

Geosci. Model Dev. Discuss., https://doi.org/10.5194/gmd-2018-41
Manuscript under review for journal Geosci. Model Dev.
Discussion started: 15 March 2018

738 **Figure 6**

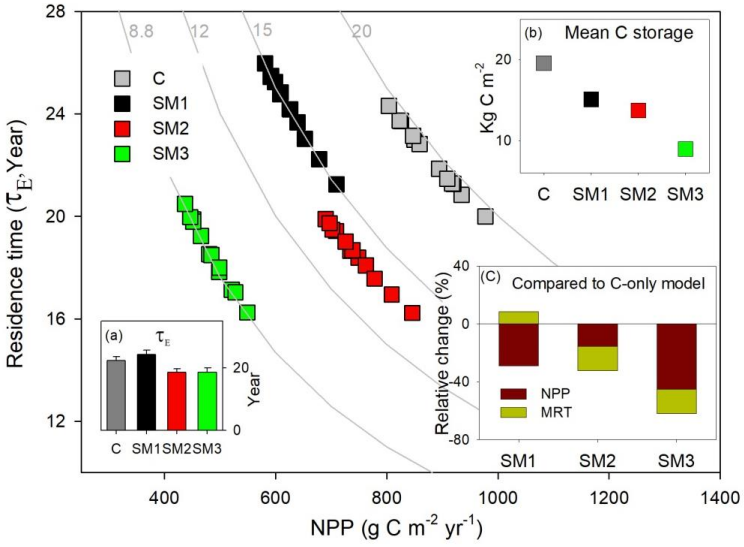

739

740 **Figure 6.** Simulation of annual ecosystem carbon storage capacity for 1996 to 2006 at Duke
741 Forest by carbon in flux (NPP, x axis) and ecosystem residence time (τ_E, y axis) in TECO model
742 framework with three carbon-nitrogen coupling schemes (SM1, SM2 and SM3) and in TECO C-
743 only model (C). The hyperbolic curves represent constant values (shown across the curves) of
744 ecosystem carbon storage capacity. Inset (a), ecosystem carbon residence time (τ_E) in SM1, SM2,
745 SM3 and C-only model; inset (b), mean ecosystem carbon storage simulated among SM1, SM2,
746 SM3 and C-only model; inset (c), relative change of NPP and ecosystem residence time
747 simulated among three schemes compared with in C-only model.

748

Geosci. Model Dev. Discuss., https://doi.org/10.5194/gmd-2018-41
Manuscript under review for journal Geosci. Model Dev.
Discussion started: 15 March 2018

749 **Figure 7**

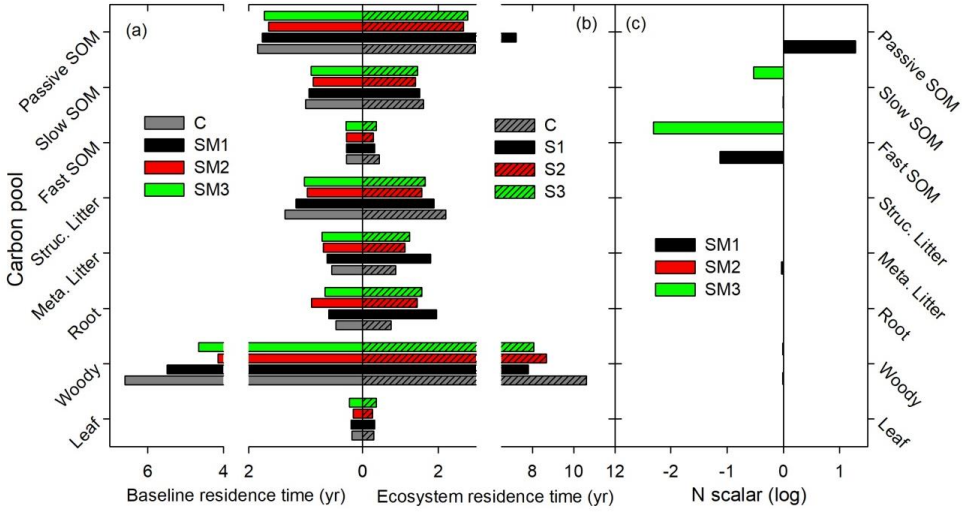

750

751 **Figure 7.** Determination of carbon-pool residence times based on traceability framework in
752 TECO C-N model with three C-N coupling schemes (SM1, SM2 and SM3) and TECO C-only
753 model (C). Panel (a), baseline residence time; panel (b), mean residence time, and panel (c),
754 nitrogen scalar.

755

Geosci. Model Dev. Discuss., https://doi.org/10.5194/gmd-2018-41
Manuscript under review for journal Geosci. Model Dev.
Discussion started: 15 March 2018

Figure 8

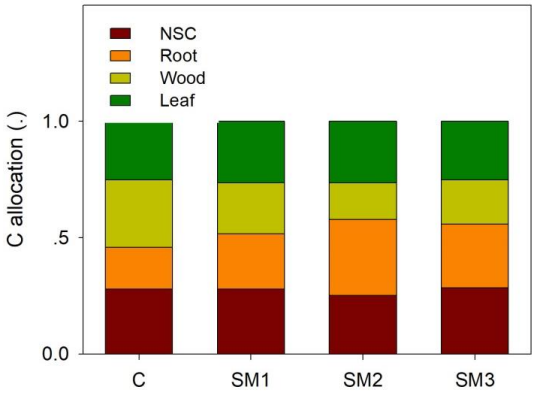

Figure 8. Coefficients of partitioning of NPP to nonstructural C (NSC), root, woody and leaf in C-only model (C) and C-N coupling model with three schemes (SM1, SM2 and SM3).

Geosci. Model Dev. Discuss., https://doi.org/10.5194/gmd-2018-41
Manuscript under review for journal Geosci. Model Dev.
Discussion started: 15 March 2018

762 **Figure 9**

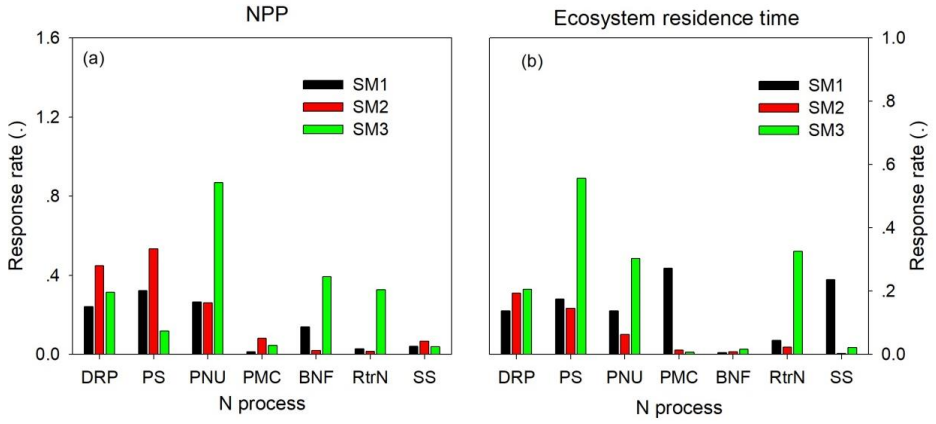

763

764 **Figure 9.** The sensitivity of nitrogen processes to NPP (panel a) and ecosystem residence time
765 (τ_E, panel b) among three carbon-nitrogen coupling schemes (SM1, SM2 and SM3). DRP, down-
766 regulation photosynthesis; PS, plant tissue C:N ratio; PNU, plant N uptake; PMC: plant and
767 microbe competition; BNF, biological N fixation; RtrN, re-tranlocation N; SS, soil pool C:N
768 ratio.

769